For high-spin iron(III), $a_i/g_n\beta_n \approx -220$ kOe/spin. At large values of H_0/T, the projection of the total spin on the magnetic field, $\langle S_{Tz} \rangle$, approaches $^5/_2$. For the $|S_T = {}^5/_2, S_{Tz} = {}^5/_2\rangle$ substate, $S_{1z} = S_{2z} = 0$ and $S_{3z} = {}^5/_2$. Therefore, from eq 22, $\vec{H}_{hf}(1) = \vec{H}_{hf}(2) = 0$ kOe and $\vec{H}_{hf}(3) = -550$ kOe, in good agreement with the experiment. By comparison, the linear $[Fe_3S_4]^+$ cluster referred to above[47d] has an $|S_T = {}^5/_2, S_p = 5\rangle$ ground state. In this case, all the $\langle S_{iz} \rangle$ values in the $\langle S_{Tz} = {}^5/_2 \rangle$ sub-level are nonzero, resulting in two magnetic subsites with 2:1 intensity ratio and nonzero magnetic hyperfine fields of opposite sign.

Weak $\Delta m = 0$ lines observed at ~ 5 and -4 mm/s in Figure 10 indicate a small zero field splitting of the ground state of the cluster. This finding may partly explain the previously noted disagreement between the observed and calculated susceptibilities at very low temperatures (Figure 8 and Table S7).

Conclusions. A new polyimidazole ligand, TIEOH, has been synthesized and characterized. Such ligands are destined to play an increasingly important role as bioinorganic chemists strive to mimic and elucidate the physical and chemical properties of metal centers in biology.[51] The asymmetric core of the μ_3-oxo complex $[Fe_3O(TIEO)_2(O_2CPh)_2Cl_3]$ represents a topological isomer of symmetric $\{Fe_3O\}^{7+}$ units found in basic iron acetates and their analogues. The different ground states elucidated here correlate with the different geometries. Knowledge of the structural and magnetic properties of these trinuclear clusters is fundamental to understanding larger iron–oxo aggregates in which these Fe_3O units may be viewed as fundamental building blocks.[8,17,36,37] In future papers we shall describe $\{Fe_4O_2\}^{8+}$ and $\{Fe_{11}O_6(OH)_6\}^{15+}$ (see also ref 36) cores that illustrate this principle.

Acknowledgment. This work was supported by National Institutes of Health Research Grant GM 32134 (to S.J.L.) from the National Institute of General Medical Services. Some of the mass spectra were provided by the Facility supported by NIH Grant RR 00317 (Principal Investigator Professor K. Biemann) from the Biotechnology Resources Branch, Division of Research Resources. R.B.F. and G.C.P. were supported by the Office of Naval Research. The Francis Bitter National Magnet Laboratory is supported by the National Science Foundation.

Supplementary Material Available: Tables S1–S7 reporting thermal parameters, and hydrogen atom parameters for $3{\cdot}4H_2O$ and $4{\cdot}2C_6H_6$ and magnetic data for the latter compound (6 pages); tables of structure factors for $3{\cdot}4H_2O$ and $4{\cdot}2C_6H_6$ (26 pages). Ordering information is given on any current masthead page.

(51) For a recent example, see: Sorrell, T. N.; Borovik, A. S. *J. Am. Chem. Soc.* **1986**, *108*, 2479–2481. In this work the Ag(I) and Cu(I) complexes of tris[2-(1-methylimidazolyl)]methoxymethane are reported. We have independently prepared this ligand and studied its chemistry with ferric salts.[17]

Synthesis, Structure, and Spectroscopic Properties of an Unusual Copper(I) Dimer Having Imidazole Ligands. A Model for the Carbonyl Derivative of Hemocyanin and Implications for the Structure of Deoxyhemocyanin

Thomas N. Sorrell*[1] and A. S. Borovik

Contribution from the Department of Chemistry, The University of North Carolina at Chapel Hill, Chapel Hill, North Carolina 27514. *Received November 14, 1986*

Abstract: Described are the synthesis of a tris(imidazole) chelating agent, timm, and the structure of its subsequently generated Cu(I) complex. The latter species is a dimer, $[Cu(timm)^+]_2$ (**1**), and its structure is compared with those of related copper(I) dimers. We also report the solution spectroscopic and photophysical properties of several copper(I) imidazole complexes including $Cu(timm)^+$ and its carbonyl adduct $Cu(timm)CO^+$. From these data, we propose a structure for the active site in HcCO which is consistent with (1) the structure deduced from protein crystallography and EXAFS spectroscopy, (2) the photophysical behavior of HcCO, and (3) the observed stoichiometry of CO binding by deoxyHc. Crystal data for **1**: monoclinic, $a = 8.515$ (4) Å, $b = 16.133$ (5) Å, $c = 13.054$ (5) Å, $\beta = 92.38$ (4)°, $V = 1792$ (2) Å^3, space group $P2_1/c$, and $Z = 4$.

Previous studies on the electronic absorption and photophysical properties of copper(I) pyrazole complexes[2] suggested to us that a similar investigation of copper(I) imidazole complexes might be useful for probing the coordination environment of copper proteins in which the metal ions were ligated by histidine. This notion, founded on the observation that the carbonyl derivative of hemocyanin (HcCO)[3] displays a luminescence at 550 nm,[4] was strengthened by a report in 1984 of the preliminary X-ray crystal structure of deoxyhemocyanin (deoxyHc) isolated from the arthropod *Panularis interruptus*.[5] The structure shows that only three imidazole residues are within bonding distance of each copper(I) ion.

In order to compare the photophysical properties of copper(I) imidazole complexes with those for the reduced forms of hemocyanin, we focused on compounds having no ligands besides imidazole. We have previously prepared several two-coordinate Cu(I) complexes,[6] but we lacked well-defined three-coordinate species.

(1) Fellow of the Alfred P. Sloan Foundation, 1985–1987.
(2) Sorrell, T. N.; Borovik, A. S. *Inorg. Chem.*, in press.
(3) Abbreviations used in this paper include the following: Hc, hemocyanin; HcO_2, oxyhemocyanin; HcCO, the carbonyl derivative of hemocyanin; deoxyHc, deoxyhemocyanin; pz, pyrazole; im, imidazole; 1,2-DMIm, 1,2-dimethylimidazole; timm, tris[2-(1-methylimidazolyl)]methoxymethane.
(4) Finazzi-Agro, A.; Zolla, L.; Flamigni, L.; Kuiper, H. A.; Brunori, M. *Biochemistry* **1982**, *21*, 415.
(5) (a) Gaykema, W. P. J.; Hol, W. G. J.; Verijken, J. M.; Soeter, N. M.; Bok, H. J.; Beintema, J. J. *Nature (London)* **1984**, *309*, 23. (b) Linzen, B.; Soeter, N. M.; Riggs, A. F.; Schneider, H.-J.; Schartau, W.; Moore, M. D.; Yokota, E.; Behrens, P. Q.; Nakashima, H.; Takagi, T.; Nemoto, T.; Verijken, J. M.; Bak, H. J.; Beintema, J. J.; Volbeda, A.; Gaykema, W. P. J.; Hol, G. W. J. *Science (Washington, D.C.)* **1985**, *229*, 519.
(6) Sorrell, T. N.; Jameson, D. J. *J. Am. Chem. Soc.* **1983**, *105*, 6013.

0002-7863/87/1509-4255$01.50/0

Thus we have prepared a tridentate chelating ligand, timm (**3**), similar to one reported previously by Breslow.[7]

This paper describes the synthesis of timm and the structure of its subsequently prepared Cu(I) complex $[Cu(timm)^+]_2$ (**1**). The structure of **1** is compared to those of related copper(I) dimers having the ligands $HBPz_3^-$ and $HB(Me_2Pz)_3^-$ (pz = 1-pyrazolyl).[8] We also report the solution spectroscopic and photophysical properties of several copper(I) imidazole complexes including $Cu(timm)^+$ and its carbonyl adduct $Cu(timm)CO^+$ (**5**).[9] Finally, we conclude with proposals about the structure of the active site in the reduced forms of hemocyanin.

Experimental Section

All reagents and solvents were purchased from commercial sources and used as received, unless noted otherwise. The following solvents were distilled and stored under nitrogen: tetrahydrofuan (THF), from sodium–benzophenone ketyl under argon, and methanol, from $Mg(OCH_3)_2$ under nitrogen. Carbon monoxide was purified by successive passage of the gas through an acidic chromium(II) solution, concentrated H_2SO_4, NaOH pellets, and Drierite. Melting points were obtained with the use of a Fisher-Johns apparatus and are uncorrected. Flash chromatography was performed according to the general procedure of Still.[10] Analytical thin layer chromatography was done by using Analtech precoated silica gel plates. Microanalyses were performed by MicAnal Laboratory, Inc., Tucson, AZ.

^1H and ^{13}C NMR spectra were recorded on an IBM AC 200 instrument using $CDCl_3$ as the solvent. All chemical shifts are reported in parts per million (ppm) relative to an internal standard of Me_4Si. Infrared spectra were recorded on a Nicolet DX-20 FTIR spectrometer, and peaks are reported in inverse centimeters. Solution studies employed a NaCl cell with a path length of 0.1 mm.

Tris[2-(1-methylimidazolyl)]methanol (2). Under a nitrogen atmosphere, 20 mL (53 mmol) of a 2.5 M solution of *n*-butyllithium in hexanes was added to 200 mL of anhydrous diethyl ether. Over a 60-min interval, a solution of 4.3 g (53 mmol) of 1-methylimidazole in 30 mL of anhydrous diethyl ether was added dropwise. The reaction mixture was stirred for 15 min, and 70 mL of THF was then added to dissolve the lithium salt. After being cooled to −78°, the mixture was treated dropwise with 10 g (11 mmol) of methyl chloroformate in 30 mL of THF. When the addition was completed, the mixture was allowed to warm to room temperature to stir for an additional hour. The reaction was quenched with aqueous ethanol, volatiles were removed under reduced pressure, and the residue was triturated with methylene chloride to remove excess 1-methylimidazole. The crude mixture was purified by flash chromatography using 10:1 acetone–methanol as the eluent to afford 2.2 g (76%) of a pale yellow solid: mp 200–202 °C; ^1H NMR δ 4.43 (s, 9 H, $N-CH_3$), 5.20 (s, 1 H, OH), 6.90 (s, 3 H, imidazolyl C5–H), 6.93 (s, 3 H, imidazolyl C4–H); ^{13}C NMR δ 34.12 (q, N–CH3), 71.71 (s, –COH), 123.61 (d, imidazolyl C5), 126.16 (d, imidazolyl C4), 146.08 (s, imidazolyl C2).

Tris[2-(1-methylimidazolyl)]methoxymethane (timm) (3). A magnetically stirred mixture of 0.477 g (1.8 mmol) of **2** and 0.084 g (3.5 mmol) of sodium hydride in 75 mL of *N,N*-dimethylformamide (DMF) was heated at 65 °C under N_2. After 3 h, the mixture was cooled to 0 °C and treated with 0.31 g (2.2 mmol) of iodomethane. The mixture was allowed to stir for 2 days at 25 °C after which the excess NaH was destroyed with aqueous ethanol. The solution was evaporated to dryness at reduced pressure, and the crude product was purified by flash chromatography using acetone as the eluent to yield 0.144 g (28%) of a white solid. The product was further purified by recrystallization from acetone: mp 145 °C dec; ^1H NMR δ 3.46 (s, 9 H, $N-CH_3$), 3.48 (s, 3 H, $-OCH_3$), 6.91 (d, J = 1 Hz, 3 H, imidazolyl C5–H), 6.98 (d, J = 1 Hz, 3 H, imidazolyl C4–H).

{Tris[2-(1-methylimidazolyl)]methoxymethane}copper(I) Tetrafluoroborate, $[Cu(timm)]_2[BF_4]_2$ (1). In an inert-atmosphere box, 0.241 g (0.841 mmol) of **3** in 5 mL of methanol was treated with a solution of 0.264 g (0.841 mmol) of $[Cu(CH_3CN)_4]BF_4$ in 5 mL of methanol. The resulting colorless solution was evaporated to dryness under vacuum, and the residue dissolved in a minimum amount of methanol and filtered. Crystals were grown by vapor diffusion of THF into the filtered methanol solution of **1**. Anal. Calcd for $C_{14}H_{18}BCuF_4N_6O$: C, 38.51; H, 4.16; N, 19.24. Found: C, 38.55; H, 4.09; N, 19.29.

{Tris[2-(1-methylimidazolyl)]methoxymethane}silver(I) Tetrafluoroborate, $[Ag(timm)]_2[BF_4]_2$ (4). This complex was prepared as described for **1** by using $AgBF_4$ as the silver(I) precursor and crystallized by vapor diffusion of THF into a filtered methanol solution of **4**. Anal. Calcd for $C_{14}H_{18}AgBF_4N_6O$: C, 34.95; H, 3.76; N, 17.46. Found: C, 34.91; H, 3.78; N, 17.29.

Conductivity Studies. All conductivity measurements were made in methanol (Burdick-Jackson Laboratories) which was distilled from $Mg(OCH_3)_2$ under nitrogen. The conductivity was measured with a Copenhagen Radiometer (Type CDM 2d) conductivity meter. The specific conductance, κ, was obtained from the relationship

$$\kappa = L(A/l)^{-1} \quad (1)$$

where L is measured conductance and A/l is the cell constant.[11] The equivalent conductance was determined from eq 2, where Λ is the

$$\Lambda = 1000\kappa(C)^{-1} \quad (2)$$

equivalent conductance and C is the concentration of the sample in equivalents per liter. The conductance data are included in the supplementary material (Tables S1 and S2).

Spectroscopic Studies. For lifetime, emission, and absorption experiments, high-purity methanol from Burdick-Jackson Laboratories and absolute ethanol were used. The alcohols were further purified by distillation under nitrogen from their respective magnesium alkoxides and stored under nitrogen. All samples were prepared under an inert atmosphere (<1 ppm of oxygen and H_2O) unless otherwise noted.

Absorption Measurements. Absorption spectra of the complexes in methanol were obtained by using a Hewlett-Packard 8450A diode array spectrophotometer. A 0.005-cm path length suprasil cell was used to minimize solvent absorption. Carbon monoxide was added to the atmosphere above the samples by slow passage of the gas through a syringe needle for 5–10 min.

Emission Studies. Emission spectra were obtained on a SLM 8000 photoncounting spectrofluorimeter and were corrected for detector sensitivity with use of data and programs supplied by the manufacturer. Low-temperature (77 K) emission spectra of the complexes in 1:4 methanol–ethanol glasses were obtained with use of cylindrical quartz-tip Dewar flask. Samples were prepared by quartz tubes that were sealed under nitrogen. Excitation spectra were corrected for lamp intensity deviations ratiometrically by using a concentrated solution of Rhodamine 6G as the standard. The standard was housed in a triangular suprasil cell to prevent self absorption.

Lifetimes. Emission lifetimes were determined by laser flash photolysis with the defocused 266-nm output (fourth harmonic) of a pulsed Quanta-Ray YAG laser as the excitation source (pulse width ca. 4 ns). Emission intensity as a function of time following excitation was monitored at right angles to the excitation pulse with an EMI Genocom Model RFI/S housing attached to a Bausch & Lomb 33-86-02 monochromator. The current output from the photomultiplier was dropped across a 50-Ω resistor. The voltage vs. time signal was acquired with a Tektronix 7623A oscilloscope, and the waveform was photographed by using a Polaroid camera. The data used for lifetime were the average result of approximately 200 decay traces. The average decay traces were digitized on a Commodore 8032 computer using a Hewlett-Packard (09872-60066) fiber optic digitizer. Lifetimes were obtained by least-squares analyses of the first-order decay plots of ln (I) vs. time (I = intensity). Samples for lifetime measurements were prepared and sealed under a nitrogen atmosphere as described above for the emission spectra. No observable differences in the lifetimes were found when freeze–pump–thaw degassed samples were used.

X-ray Data Collection for 1. A regularly shaped crystal approximately 0.25 mm on a side was mounted on the end of a glass fiber and a preliminary diffractometer search revealed monoclinic symmetry. Systematic absences were observed which were consistent with the space group $P2_1/c$. Diffraction data were collected at 293 K on an Enraf-Nonius CAD-4 diffractometer using Mo Kα radiation (0.7107 Å) from a graphite crystal monochromator. The unit cell constants were derived from a least-squares refinement of 24 reflections. The ω-2θ scan technique was used to record the intensities. Peak counts were corrected for background counts, which were obtained by extending the final scan by 25% at each end to yield net intensities, I, which were assigned standard deviations calculated with a conventional p factor of 0.01. Intensities were corrected for Lorentz and polarization effects and showed no decay during collection as monitored by the intensities of three standard reflections. The data were further corrected for absorption effects by using an empirical

(7) Tang, C. C.; Davalian, D.; Huang, P.; Breslow, R. *J. Am. Chem. Soc.* **1978**, *100*, 3918–3922.

(8) Meali, C.; Arcus, C. S.; Wilkinson, J. L.; Marks, T. J.; Ibers, J. A. *J. Am. Chem. Soc.* **1976**, *98*, 711–718.

(9) A preliminary account of this work has already appeared: Sorrell, T. N.; Borovik, A. S. *J. Am. Chem. Soc.* **1986**, *108*, 2479–2481.

(10) Still, W. C.; Kahn, M.; Mitra, A. *J. Org. Chem.* **1978**, *43*, 2923.

(11) The conductivity cell constant was determined by using a standard aqueous KCl solution.

Table I. Crystallographic Details for $[Cu(timm)]_2[BF_4]_2$

formula	$C_{14}H_{18}CuBF_4N_6O$
temp, K	293
space group	$P2_1/c$
a, Å	8.515 (4)
b, Å	16.133 (5)
c, Å	13.054 (5)
β, deg	92.38 (4)
V, Å^3	1792
Z	4
ρ(calcd), g/cm^3	1.62
collectn range	$\pm h,+k,+l$
	$2.0° \le 2\theta \le 54.0°$
transmissn factors	
min	0.85
max	1.00
abs coeff, cm^{-1}	13.3
no. of data	4069
no. of data [$I \ge 3\sigma(I)$]	1917
no. of variables	244
R	0.060
R_w	0.055

Table II. Final Positional Parameters for $[Cu(timm)]_2[BF_4]_2$

atom	x	y	z
Cu	0.0732 (1)	0.08866 (5)	0.01506 (6)
F1	0.4798 (6)	0.2407 (4)	0.5573 (5)
F2	0.4620 (7)	0.1573 (4)	0.4208 (5)
F3	0.5253 (3)	0.1094 (5)	0.5597 (7)
F4	0.6873 (7)	0.1806 (4)	0.5006 (5)
O	0.0518 (5)	−0.0332 (3)	0.3331 (3)
N1	0.2223 (6)	0.0303 (4)	0.1186 (4)
N2	−0.1224 (6)	−0.1377 (3)	0.1122 (4)
N3	−0.0938 (6)	0.0807 (3)	0.1127 (4)
N1A	0.2758 (6)	−0.0956 (4)	0.1778 (4)
N2A	−0.1178 (6)	−0.1748 (3)	0.2757 (4)
N3A	−0.2251 (6)	0.0513 (3)	0.2489 (4)
C1	0.0152 (7)	−0.0370 (4)	0.2262 (4)
C2	0.1402 (10)	0.0367 (5)	0.3666 (6)
C1A	0.1655 (7)	−0.0347 (4)	0.1681 (5)
C1B	0.3743 (8)	0.0093 (5)	0.0975 (6)
C1C	0.4074 (8)	−0.0664 (5)	0.1318 (6)
C1D	0.2626 (9)	−0.1770 (5)	0.2251 (6)
C2A	−0.0712 (7)	−0.1176 (4)	0.2068 (4)
C2B	−0.2063 (8)	−0.2108 (4)	0.1207 (5)
C2C	−0.2019 (8)	−0.2335 (4)	0.2190 (5)
C2D	−0.0851 (9)	−0.1826 (5)	0.3858 (5)
C3A	−0.0965 (7)	0.0326 (4)	0.1953 (5)
C3B	−0.2235 (8)	0.1323 (4)	0.1153 (5)
C3C	−0.3024 (8)	0.1143 (4)	0.1987 (6)
C3D	−0.2827 (10)	0.0129 (6)	0.3414 (6)
B	0.541 (1)	0.1836 (7)	0.4982 (9)

correction based on psi scan data. Crystal data are given in Table I (crystallographic details).

Structure Determination and Refinement. A three-dimensional Patterson synthesis was used to locate the copper atom positions, and a series of Fourier maps revealed the remaining non-hydrogen atom positions. The refinement was effected by full-matrix least-squares techniques. The function minimized was $\sum w(|F_o| - |F_c|)^2$ where $|F_o|$ and $|F_c|$ are the observed and calculated structure amplitudes, respectively, and the weight, w, is $4F_o^2/\sigma^2(F_o^2)$. Programs used for the structure solution and refinement were supplied as a package by Enraf-Nonius. Atomic scattering factors for the non-hydrogen atoms were taken from ref 12 and those for hydrogen atoms from ref 13. Calculated, idealized hydrogen atom positions were included in the structure factor calculations but were not refined. The final weighted R factor (on F) was 0.055, and the unweighted R factor was 0.060. Final positional parameters are given in Table II, and the distances and angles are listed in Table III.

(12) *International Tables for X-ray Crystallography*; Kynoch: Birmingham, England, 1974; Vol. IV.
(13) Stewart, R. F.; Davidson, E. R.; Simpson, W. T. *J. Chem. Phys.* **1965**, *42*, 3175–3178.
(14) (a) Woolery, G. L.; Powers, L.; Winkler, M.; Solomon, E. I.; Spiro, T. G. *J. Am. Chem. Soc.* **1984**, *106*, 86–92. (b) Co., M. S.; Hodgson, K. O. *J. Am. Chem. Soc.* **1981**, *103*, 3200–3202.

Table III. Bond Distances and Angles for $[Cu(timm)]_2[BF_4]_2$

Distances, Å

Cu–N1	2.045 (3)	Cu–N2	1.903 (3)	Cu–N3	1.953 (3)
N1–C1A	1.333 (5)	N1–C1B	1.377 (5)	N2–C2A	1.332 (4)
N2–C2B	1.387 (5)	N3–C3A	1.329 (4)	N3–C3B	1.386 (5)
O–C1	1.418 (4)	O–C2	1.415 (5)	N1A–C1A	1.362 (5)
N1A–C1C	1.376 (6)	N1A–C1D	1.458 (6)	N2A–C2A	1.359 (4)
N2A–C2C	1.383 (5)	N2A–C2D	1.458 (5)	N3A–C3A	1.357 (5)
N3A–C3C	1.364 (5)	N3A–C3D	1.460 (5)	C1–C1A	1.515 (5)
C1–C2A	1.511 (5)	C1–C3A	1.515 (5)	C1B–C1C	1.326 (7)
C2B–C2C	1.334 (6)	C3B–C3C	1.335 (6)	B–F1	1.324 (8)
B–F2	1.264 (7)	B–F3	1.450 (12)	B–F4	1.245 (7)
Cu–Cu′	3.139 (1)				

Angles, deg

N1–Cu–N2	127.94 (14)	N1–Cu–N3	89.27 (14)
N2–Cu–N3	142.24 (14)	Cu–N1–C1A	117.01 (28)
Cu–N1–C1B	122.99 (31)	C1A–N1–C1B	105.45 (40)
Cu–N2–C2A	129.18 (27)	Cu–N2–C2B	123.80 (28)
C2A–N2–C2B	106.42 (33)	Cu–N3–C3A	127.31 (29)
Cu–N3–C3B	125.38 (29)	C3A–N3–C3B	106.86 (33)
C1–O–C2	115.51 (32)	C1A–N1A–C1C	106.45 (39)
C1A–N1A–C1O	128.66 (37)	C1C–N1A–C1D	124.88 (42)
C2A–N2A–C2C	105.67 (33)	C2A–N2A–C2D	131.43 (37)
C2C–N2A–C2D	122.78 (36)	C3A–N3A–C3C	107.57 (37)
C3A–N3A–C3D	129.60 (40)	C3C–N3A–C3D	122.80 (41)
O–C1–C1A	109.64 (32)	O–C1–C2A	106.69 (30)
O–C1–C3A	109.88 (31)	C1A–C1–C2A	110.63 (33)
C1A–C1–C3A	112.49 (33)	C2A–C1–C3A	107.33 (31)
N1–C1A–N1A	110.46 (36)	N1–C1A–C1	126.39 (39)
N1A–C1A–C1	121.98 (36)	N1–C1B–C1C	110.32 (46)
N1A–C1C–C1B	107.32 (44)	N2–C2A–N2A	110.80 (34)
N2–C2A–C1	120.19 (33)	N2A–C2A–C1	128.85 (34)
N2–C2B–C2C	108.44 (38)	N2A–C2C–C2B	108.66 (36)
N3–C3A–N3A	109.27 (36)	N3–C3A–C1	128.03 (37)
N3A–C3A–C1	122.59 (37)	N3–C3B–C3C	108.53 (38)
N3A–C3C–C3B	107.75 (39)	F1–B–F2	119.37 (59)
F1–B–F3	101.76 (88)	F1–B–F4	115.44 (63)
F2–B–F3	96.16 (73)	F2–B–F4	120.43 (82)
F3–B–F4	94.01 (70)		

Scheme I[a]

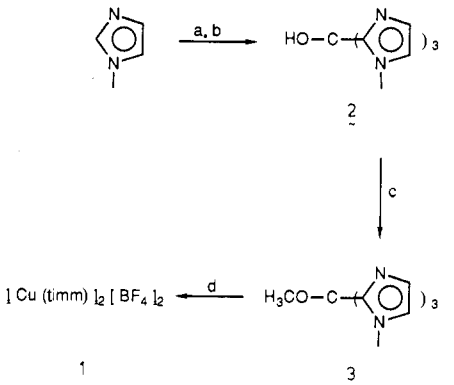

[a] a, *n*-BuLi, anhydrous ethyl ether, 25 °C, 75 min; b, $ClCOOCH_3$, THF, −78 °C; c, NaH, then CH_3I, DMF, 25 °C, 48 h; d, $Cu(CH_3CN)_4BF_4$, CH_3OH/THF, N_2, 30 °C, 7 days.

Structure factors, thermal parameters, and hydrogen atom positions are included in the supplementary material (Tables S3–S5).

Results and Discussion

Synthesis. Even though the crystal structure shows three histidyl imidazole groups bound to copper ions in deoxyHc,[5] the results of EXAFS studies have been interpretted differently, suggesting that the copper(I) ions in the protein might be two- *or* three-coordinate. Using the model compound approach to distinguish between these two possibilities requires well-defined complexes. In order to proceed then, we required a tridentate ligand to prevent formation of the very stable, linear two-coordinate complex in solution.[6] Tris[2-(1-methylimidazolyl)]methoxymethane (timm) and its corresponding copper(I) complex were synthesized as

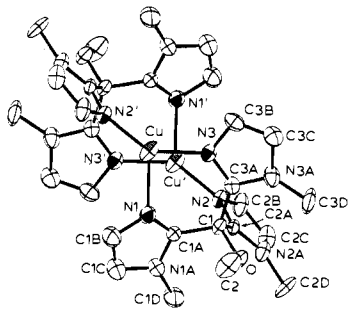

Figure 1. Structure of the $[Cu(timm)]_2^{2+}$ cation showing 40% probability thermal elipsoids. The Cu–Cu distance is 3.139 (1) Å. Bond distances and angles are given in Table III.

outlined in Scheme I. Methyl chloroformate was treated with the 2-lithio-1-methylimidazole to produce alcohol **2**, which was converted to timm by methylating the hydroxyl group with iodomethane.[15] The colorless, crystalline Cu(I) and Ag(I) complexes were readily synthesized from $[Cu(CH_3CN)_4]BF_4$ and $AgBF_4$ in methanol, respectively. Although neither complex is air-sensitive in the solid state, each was stored and manipulated in an inert atmosphere.

Solid-State Structure of $[Cu(timm)]_2[BF_4]_2$ (1). The complex crystallized from methanol–THF in the monoclinic space group $P2_1/c$. Crystal data are given in Table I, final positional parameters are listed in Table II, and bond distances and angles are collected in Table III. The structure of the cation is presented in Figure 1.

As mentioned above, timm was designed to yield a tris(imidazole) ligand set. Figure 1 illustrates that **1** crystallizes as a three-coordinate copper(I) dimer which incorporates two timm ligands. Each copper(I) ion is ligated by three imidazole groups with two donors coming from one tridentate ligand and the third donor from the other. The copper ions are separated by 3.139 Å and the dimer sits on a crystallographic inversion center. The geometry about each copper atom can be described as distorted trigonal in which the Cu atom sits 0.079 Å out of the plane described by N1, N2′, N3. The Cu–N distances are similar to those reported for other three-coordinate copper(I) complexes.[16] The relatively small angle of 89.2° formed by N1–Cu–N3 results from the rigidity imposed on the complex by the chelating nature of timm.

Instead of being unique, the unusual dimeric structure of **1** actually provides an additional example of this type of coordination by a tripod ligand. Related complexes having either the hydridotris(1-pyrazolyl)borate or the hydridotris(3,5-dimethyl-1-pyrazolyl)borate ligand have been characterized by Ibsers et al.;[8] and a comparison of those structures with the one described here is relevant in probing the binuclear structure of hemocyanin. For the complexes characterized in the previous study, the Cu···Cu separation is only 2.5 or 2.6 Å; and for the ligand derived from pyrazole itself, a nitrogen atom from each ligand bridges the copper ions. An hypothesis based on those results, presented at the time, was that unusually short Cu–Cu distances and bridging imidazole donors might be found in type III copper proteins. However, we now know from the preliminary structure of deoxyHc that the coppers are about 3.8 Å apart, and the histidine residues do not bridge.[5]

The structure reported here is like that found for $\{Cu[(3,5\text{-}Me_2Pz)_3BH]\}_2^{2+}$ and demonstrates that imidazole bridging is not necessary for stabilization of Cu(I) in synthetic complexes or, most likely, in proteins. Thus, an imidazole chelate that is geometrically identical with the hydridotris(1-pyrazolyl)borate ion adopts a similar type of ligation mode; however, no bridging by the nitrogen atom is observed, and the Cu···Cu distance of 3.1 Å is significantly longer.[17] This result is not unexpected with our current knowledge of the coordination chemistry of Cu(I) complexes ligated by nitrogenous donors. Mononuclear and unbridged dinuclear two-,[6,18] three-,[16] and four-coordinate[19] complexes are now viewed as common entities, although such species were rare 10 years ago.[20]

Moreover, the formation of dimeric Cu(I) complexes incorporating ligands designed to form mononuclear species is apparently not uncommon. We reported such a case for a two-coordiante complex;[18] and recently, an example involving formation of a dimeric four-coordinate Cu(I) species was published.[16b] Given the substitution lability of the Cu(I) ion, monomer–dimer equilibria undoubtedly occur in solution. In each of these cases, the dimeric complex is apparently the less soluble; therefore it is the one isolated.

Table IV. Spectroscopic Data for Imidazole Ligands and Complexes

complex or ligand	$\lambda^{a,b}$ (ϵ)^c	$\lambda_{em}^{b,e,f}$	$\lambda_{ex}^{b,e}$	τ^g
timm	255 (23.7)			
$Cu(timm)BF_4$	232 (28.9)	590	253	160
	285 (3.75)		285	
$[Cu(timm)CO][BF_4]^d$	216 (37.9)	550	273	38.4
	238 (sh)			
	276 (6.13)			
$Ag(timm)BF_4$	219 (sh)			
	234 (20.7)			
2-MeIm	201 (9.66)			
$Cu(2\text{-}MeIm)_2BF_4$	207 (28.2)			
1,2-DMIm	205 (8.59)			
$Cu(1,2\text{-}DMIm)_2BF_4$	205 (33.6)			

[a] In methanol. [b] nm. [c] mM^{-1} cm^{-1}; sh = shoulder. [d] ν_{CO} = 2080 cm^{-1}. [e] 1:4 methanol–ethanol glass. [f] Excitation wavelength, 300 nm. [g] s × 10^{-6}.

Solution Structure. Although complex **1** is a dimer in the solid state, there is no reason to expect that it retains this structure in solution, especially given the precedent for dissociation in the case of the dimer ligated by hydridotris(3,5-dimethyl-1-pyrazolyl)borate.[8] An advantage of studying the present system is that the charge on the complex allowed us to investigate the solution properties by conductivity measurements. If **1** and its carbonyl adduct **5**[21] were dimeric in solution, they would possess properties similar to those found for a 2:1 electrolyte, whereas if dissociation occurs to yield a monomeric copper(I) species, the conductance of the solution would be like that for a 1:1 electrolyte.

The conductance data for **1**, **5**, and 1:1 and 2:1 electrolyte standards are included in the supplementary material (Tables S1 and S2), and the electrolytic behavior was determined from conductivity measurements using the Onsager relationship.[22,23] Onsager plots for **1** and **5** are included in the supplementary material and show that both complexes are 1:1 electrolytes, suggesting that the dominant species in methanolic solution is a monomer.[24] Thus, the dimer that exists in the solid state dis-

(15) All attempts, including hydrogenolysis, to convert alcohol **2** to its corresponding alkane were unsuccessful.

(16) (a) Sorrell, T. N.; Malachowski, M. R. *Inorg. Chem.* **1983**, *22*, 1883 and references therein. (b) Nelson, S. M.; Lavery, A.; Drew, M. G. B. *J. Chem. Soc., Dalton Trans.* **1986**, 911–920 and references therein.

(17) Another case has been reported in which a potentially three-coordinate Cu(I) complex forms a metal-bonded dimer rather than adopting a nonplanar monomeric structure: Gagnê, R. R.; Kreh, R. P.; Dodge, J. A.; Marsh, R. E.; McCool, M. *Inorg. Chem.* **1982**, *21*, 254–261.

(18) Sorrell, T. N.; Jameson, D. J. *J. Am. Chem. Soc.* **1982**, *104*, 1053–2054 and references therein.

(19) Sorrell, T. N.; Jameson, D. J. *Inorg. Chem.* **1982**, *21*, 1014–1019 and references therein.

(20) Ten years ago, only very few two- and three-coordinate Cu(I) complexes had been reported: Lewin, A. H.; Cohen, I. A.; Michl, R. *J. Inorg. Nucl. Chem.* **1974**, *36*, 1951–1957.

(21) The carbonyl derivative is generated by addition of CO to a methanol solution of $Cu(timm)^+$. Attempts to isolate this adduct were unsuccessful since the dimer, **1**, is much less soluble.

(22) Geary, W. J. *Coord. Chem. Rev.* **1971**, *5*, 1141.

(23) The values for Δ_o were obtained from least-squares analyses of Δ vs. $(C)^{1/2}$ plots. The values of b were also determined by least-squares analysis from the Onsager plots: $Cu(timm)BF_4$, 2687 (0.9979); $[Cu(timm)CO][BF_4]$, 2513 (0.9966); $NaBF_4$ (22 °C) 2007 (0.9929); $NaBF_4$ (27 °C) 2245 (0.9925); $Co(bpy)_3[BF_4]_2$ 4658 (0.9909). The units of slope are S·equiv$^{-1.5}$·cm^2·L (note S = Ω^{-1}).

(24) The difference between the slopes for the compounds examined arises because the mobilities in methanol are not identical even though the charge is.

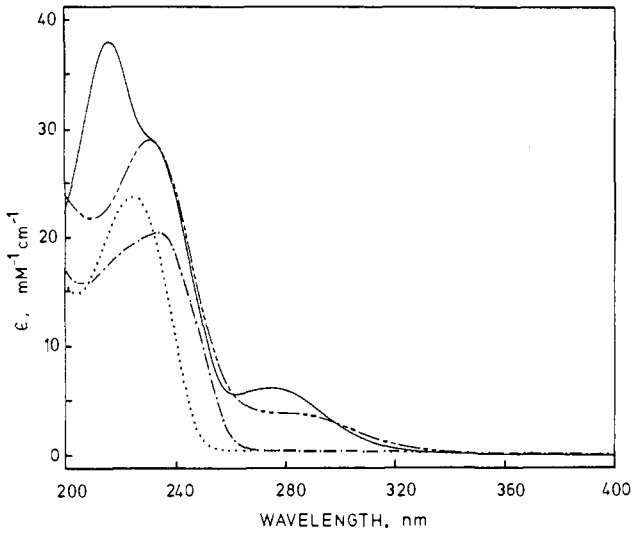

Figure 2. Electronic absorption spectra of Cu(timm)$^+$ (- - -), Cu(timm)CO$^+$ (—), timm (···), and Ag(timm)$^+$ (-·-) in methanol solutions at room temperature.

sociates into Cu(timm)$^+$ units in solution and most likely adopts the structures depicted in eq 3 depending on whether CO is present.

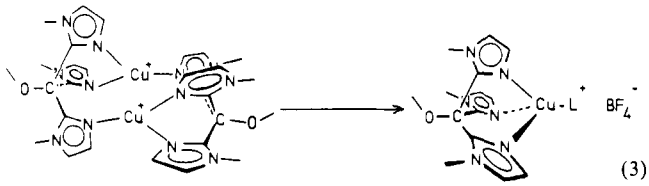

(3)

L = MeOH, CO

We assume that methanol binds in the fourth coordination site in the absence of CO since there are no examples of three-coordinate, trigonal-pyramidal Cu(I) complexes. Structurally this would be analogous to a nonplanar carbocation which is energetically much less favorable than the planar form.

The proposed structure for the CO adduct is supported by the findings for the analogous copper(I) carbonyl complex made with the hydridotris(1-pyrazolyl)borate ligand. The structure of that species, confirmed by X-ray analysis,[25] has three pyrazole groups from the tridentate ligand and a molecule of CO bound to the copper(I) ion in a tetrahedral arrangement.

Spectroscopic Studies. Absorption and emission data for several M(I) imidazole complexes (M = Cu, Ag) are given in Table IV. The electronic spectrum for Cu(timm)$^+$, shown in Figure 2, is dominated by intense transitions in the UV region of the spectrum. These transitions are the Cu(I) → imidazole charge-transfer transitions, and the band at 285 nm corresponds to the dσ^* → π^* transitions while the higher energy absorption at 232 nm is assigned to the dπ → π^* transitions.[2] Unlike those for copper(I) pyrazole complexes, the dπ → π^* band is not resolvable from the ligand-centered transitions because the π^* orbitals of imidazole are at relatively high energy compared to those of pyrazole. This in turn causes the MLCT bands to appear at higher energy. Included in Figure 2 is the absorption spectrum of Ag(timm)$^+$ (**4**) which shows the expected shift to higher energy of the MLCT transitions. These results mirror the finding for the two-, three-, and four-coordinate pyrazole complexes where the blue shift of the MLCT transitions are a result of the higher oxidation potential of the Ag(I) ion relative to Cu(I).[2] For complex **4**, the band at 240 nm, which predominantly comprises the ligand centered absorptions, is clearly unsymmetrical, suggesting the possibility that some MLCT transitions may occur in this energy region.

Cu(timm)$^+$ reacts with CO in methanol[21] as shown by the appearance of a strong CO stretch at 2080 cm^{-1} in the infrared

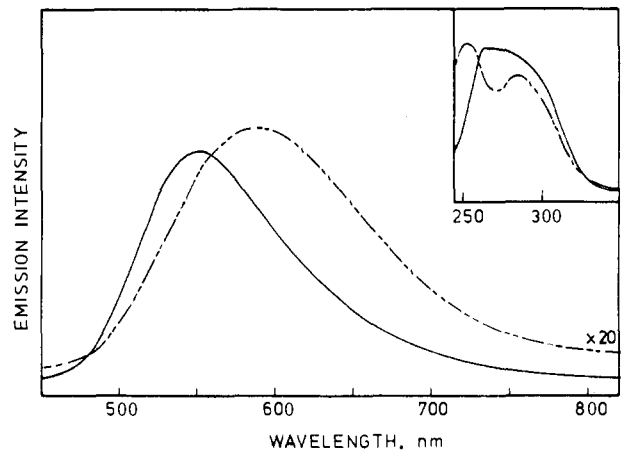

Figure 3. Corrected emission spectra of Cu(timm)$^+$ (- - -) and Cu(timm)CO$^+$ (—) in a 1:4 methanol–ethanol glass at 77 K. The insert is the corresponding corrected excitation spectra.

region. As presented in Figure 2, the binding of CO shifts the MLCT transitions to higher energy, and the position of the dπ → π^* band is shifted to a greater extent (232 → 216 nm; ΔE = 3200 cm^{-1}) than the dσ^* → π^* transitions (285 → 276 nm; ΔE = 1100 cm^{-1}). This is expected since binding a good π-acid like CO should have a greater stabilizing effect on the dπ orbitals because of back-bonding. While it is known that the back-bonding ability of Cu(I) is relatively poor,[26] the CO stretching frequency of Cu(timm)CO$^+$ relative to that of free CO suggests that back-bonding does occur, at least to an extent that should affect the energies of the dπ orbitals. The shoulder at 230 nm is assigned as the π → π^* transitions of the imidazole rings, and those are unaffected by the bindng of carbon monoxide.

Included in Table IV are absorption data for some two-coordinate Cu(I) imidazole complexes. Those complexes have intense, high-energy absorption bands centered at approximately 210 nm, which, on the basis of comparisons with the absorption properties of the unbound ligand and copper(I) pyrazole complexes, we assign to both MLCT and ligand-centered transitions.

The photophysical data for the copper(I) imidazole complexes are summarized in Table IV, and the corrected emission and excitation spectra for Cu(timm)$^+$ and Cu(timm)CO$^+$ at 77 K are shown in Figure 3.[27] Both complexes show broad structureless bands that are characteristic of emission from MLCT states.[28] The emission from Cu(timm)CO$^+$ shifts 1300 cm^{-1} to higher energy relative to Cu(timm)$^+$ (550 vs. 592 nm). this is similar to the energy difference observed for the corresponding MLCT transitions in the absorption spectrum (vide supra). The lifetimes of the excited states are in the microsecond range which suggests that these states have substantial triplet character. Hence, the emission from both complexes is assigned as originating from triplet, MLCT excited states (^{3}d-π^*). Particularly noteworthy is that the luminescence at 550 nm observed for Cu(timm)CO$^+$ occurs at the same energy as that for HcCO.

In contrast to the results found for the Cu(I) pyrazole complexes, both the emission and absorption transitions for Cu(timm)$^+$ shift to *higher* energy upon binding of CO. The major cause for this discrepancy is that Cu(timm)$^+$, probably as a methanol adduct, has the same geometry in solution as does its carbonyl derivative **5**. The position of the imidazole rings is restricted by the chelating nature of the tridentate timm ligand that prevents the complex from adoptng a planar geometry (vide supra). The orbials influencing the luminescence are therefore similar, and their energies are affected only by the magnitude of back-bonding to CO in **5**. This differs from the previously reported pyrazole species in which the complex is planar when three-coordinate but tetrahedral when CO is bound.[2]

(25) Churchill, M. R.; DeBoer, B. G.; Rotella, F. J.; AbuSalah, O. M.; Bruce, M. I. *Inorg. Chem.* **1975**, *14*, 2051–2056.

(26) Thompson, J. S.; Whitney, J. F. *Inorg. Chem.* **1984**, *23*, 2813.

(27) No emission was observed for any of the Cu(I) imidazole complexes at room temperature in methanol.

(28) Meyer, T. J. *Pure* Appl. *Chem.* **1986**, *58*, 1193.

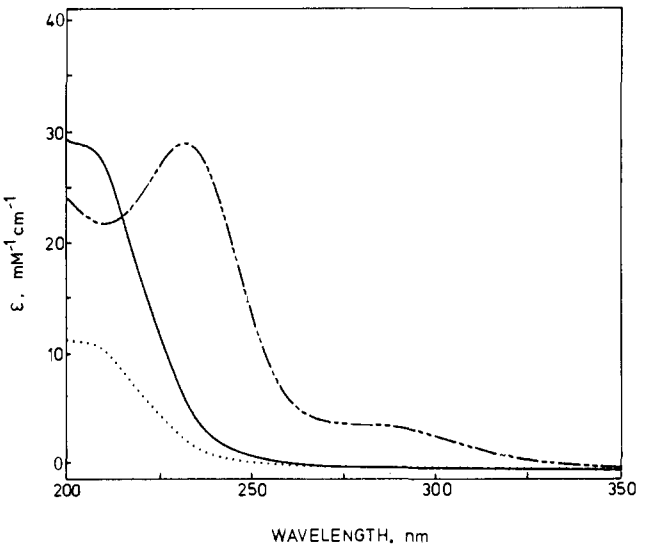

Figure 4. Electronic absorption spectra for $Cu(2\text{-}MeIm)_2^+$ (—), $Cu(timm)^+$ (- - -), and 2-MeIm (···) in methanol solutions at room temperature.

In contrast to $Cu(timm)^+$, the two-coordinate imidazole complexes do not luminescence when excited at 300 nm. A comparison in Figure 4 of the electronic spectra shows why, namely, that there are no MLCT bands in the 300-nm region for $Cu(2\text{-}MeIm)_2^+$.

Biological Implications. The complexes presented here represent an improvement over the pyrazole complexes studied earlier[2] because they incorporate the biologically important imidazole ligand. From a comparison of the properties of $Cu(timm)^+$, $Cu(timm)(CO)^+$, and two-coordinate Cu(I) imidazole complexes, we can draw several conclusions about the structure of the active site in the reduced derivatives of hemocyanin.

HcCO. Hemocyanin binds only one CO molecule per two Cu(I) ions;[29] therefore, the coordination environments of the two copper ions are probably somewhat different from one another. We propose that the copper ion that binds the carbon monoxide has three histidyl imidazole ligands and the other copper ion is essentially two-coordinate. This proposal is consistent with (i) our previous demonstration that three ligands are necessary for copper(I) to bind CO and explains why only one CO ligand is bound per active site in Hc and (ii) our observation that the luminescence for HcCO at 550 nm can be reproduced with a Cu(I) complex havng only three imidazole ligands and CO.

Furthermore, we speculate that the active site in HcCO is in a hydrophobic environment, shielded from solvent by the protein, since emission from HcCO is observed at room temperature. In contrast, synthetic copper(I) imidazole complexes luminescence only when isolated in a glass. As shown previously, solvent coordination in the excited state can quench the luminescence from Cu(I) complexes.[2,30] Zolla and co-workers have recently reported that the carbonyl derivative of the half-apo form of hemocyanin (one Cu(I) ion per active site) does not luminesce, even though the single copper(I) ion still should be bound by one CO and three imidazole ligands.[31] They have postulated that the second copper ion, which does not have a CO group bound, is essential for emission to occur from the active site. On the basis of results presented here, it appears unlikely that the second copper(I) ion is involved *directly* in the photophysical processes associated with the Cu(I)–CO moiety. It may be that the absence of the second copper(I) ion causes a conformational change that is localized at the active site and allows the Cu(I)–CO unit to be exposed to solvent, quenching the emission. Another possibility is that absence of the second copper(I) ion may allow tryptophan, or another amino acid, to approach the active site more easily, leading to quenching.

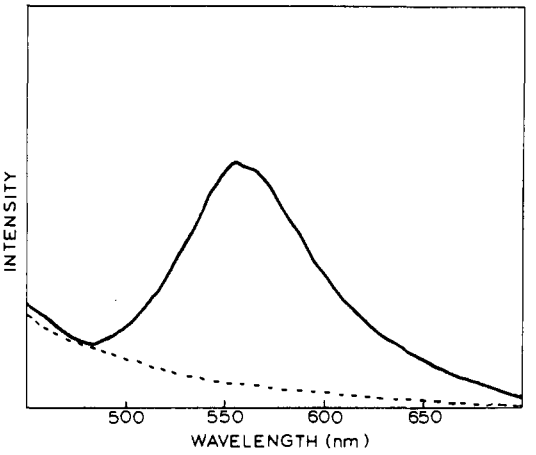

Figure 5. Emission spectra of deoxyHc (- - -) and HcCO (—) in a 5% glucose buffer glass at 77 K. The excitation wavelength is 300 nm.

DeoxyHc. On the basis of the present results, we can draw few definitive conclusions about the structure of the active site in deoxyHc that are not already apparent from the crystal structure, which shows that the copper ions are bound to three histidyl imidazole ligands.[5] If the three imidazole ligands that are near the copper ions are coordinated in a nonplanar geometry, perhaps with a water molecule bound in the fourth site, then the lack of emission for deoxyHc, even at 77 K (Figure 5), is unexpected because $Cu(timm)^+$ provides a structural analogue that *does* luminesce under those conditions. One explanation is that, in the case of the protein, the emission is quenched because of the presence of, for example, tryptophan. However, it may also be that the actual geometry about each copper ion in the protein is different from that of $Cu(timm)^+$. For instance, if the copper(I) centers in deoxyHc were closer to two-coordinate, then no emission would be observed when irradiation were carried out at 300 nm because, as demonstrated above, $Cu(Im)_2^+$ species have no absorption bands in that region (Figure 4). While we are tempted to speculate that the copper ions in deoxyHc are actually closer to two- than to three-coordinate, we recognize that alternatives such as the planar, three-coordinate or bent, two-coordinate geometries need to be evaluated first before such proposals are made. However, the lack of luminescence for deoxyHc may provide a useful probe of its active-site structure.

Acknowledgment is made to the National Science Foundation for support of this work. We thank B. P. Sullivan, T. D. Westmoreland, Prof. T. J. Meyer, and E. Kober for helpful discussions and for use of their equipment and Drs. Joseph and Celia Bonaventura for the sample of hemocyanin used to record Figure 5.

Supplementary Material Available: Conductivity data (Tables S1 and S2), final hydrogen atom positions (Table S3), thermal parameters (Table S4) and Onsager plots of $Cu(timm)^+$ and $Cu(timm)^+CO$ (6 pages); a listing of observed and calculated structure factors (Table S5) (14 pages). Ordering information is given on any current masthead page.

(29) Alben, J. O.; Yen, L.; Farrier, N. J. *J. Am. Chem. Soc.* **1970**, *92*, 4475–4476.
(30) McMillin, D. R.; Kirchoff, J. R.; Goodwin, K. V. *Coord. Chem. Rev.* **1985**, *64*, 83.
(31) Zolla, L.; Calabrese, L.; Brunori, M. *Biochim. Biophys. Acta* **1984**, *788*, 206.